



Heterogeneous & Homogeneous & Bio- & Nano-

# CHEM **CAT** CHEM

---

## CATALYSIS

### Accepted Article

**Title:** Chemo- and regioselective synthesis of arylated  $\gamma$ -valerolactones from bio-based levulinic acid with aromatics using H- $\beta$  zeolite catalyst

**Authors:** Sreedhar Gundekari and Kannan Srinivasan

This manuscript has been accepted after peer review and appears as an Accepted Article online prior to editing, proofing, and formal publication of the final Version of Record (VoR). This work is currently citable by using the Digital Object Identifier (DOI) given below. The VoR will be published online in Early View as soon as possible and may be different to this Accepted Article as a result of editing. Readers should obtain the VoR from the journal website shown below when it is published to ensure accuracy of information. The authors are responsible for the content of this Accepted Article.

**To be cited as:** *ChemCatChem* 10.1002/cctc.201801782

**Link to VoR:** <http://dx.doi.org/10.1002/cctc.201801782>

WILEY-VCH

[www.chemcatchem.org](http://www.chemcatchem.org)



## FULL PAPER

Chemo- and regioselective synthesis of arylated  $\gamma$ -valerolactones from bio-based levulinic acid with aromatics using H- $\beta$  zeolite catalystSreedhar Gundekari,<sup>[a, b]</sup> and Kannan Srinivasan <sup>\*[a, b]</sup>

**Abstract:** Catalytic coupling of biomass-based molecules to value-added chemical intermediates is an interesting area in biomass research. Arylated  $\gamma$ -valerolactones (Agvls), promising pharmaceutical intermediates that have significant biological activity, are primarily synthesized currently through petro-route. In this paper, we report successful biomass-based synthesis of Agvls using levulinic acid (LA) and oxygen or sulphur- substituted aromatics over H- $\beta$  zeolite as catalyst under solvent-free conditions. Under optimized condition, LA and anisole render 90% conversion of former with 82% yield of para-substituted  $\gamma$ -lactone. C-C bond formation followed by intra-molecular esterification is witnessed in the course of the reaction, which is highly chemo- and regioselective. Though catalyst deactivated while reuse due to deposition of organic carbon moieties as deduced from several physicochemical techniques, it could be regenerated by simple calcination.

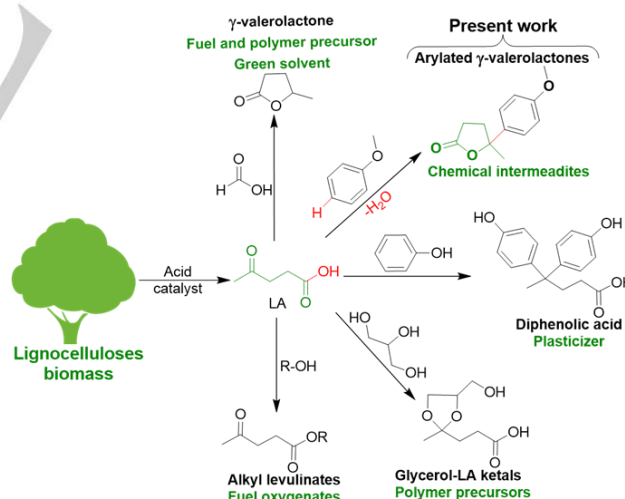
## Introduction

The ever-increasing demand for fossil fuels and petroleum-derived products is causing a depletion of the Earth's conventional fuel reserves. About 90% of today's organics are petrochemical based. This has escalated the need for alternative and renewable sources for fuels and commodity chemicals.<sup>[1]</sup> Biomass is the most promising alternative feedstock for fuels and value-added chemicals.<sup>[2]</sup> Use of biomass also increases the rural economics and results in a decrease in greenhouse gas (GHG) emissions compared to petroleum-based feedstock.<sup>[3]</sup> The major components of biomass are plant cell wall (lignocellulose) and plant seeds (triglycerides). The primary platform chemicals of lignocellulose/triglyceride biomass are sugars, alcohols, furans, alkenes, carboxylic acids, esters, carbonyl compounds, phenolics and glycerol-derived molecules which could be obtained via biological and/or chemical transformations.<sup>[4]</sup>

Catalytic transformations of biomass to organics like fuels, chemicals, polymers etc. are likely to have an immense impact on future generations.<sup>[5]</sup> Levulinic acid (LA), a biomass-derived keto carboxylic acid, serves as an important building block for valuable fuels and chemicals obtainable via catalytic transformations.<sup>[6]</sup> LA

is easily obtained from abundant waste/surplus carbohydrate (C6-Glucose/C5-Xylose) biomass like sawdust, paper mill sludge, tobacco chops, sugarcane bagasse and wheat by the acid catalysed dehydration followed by subsequent hydration using various homo/heterogeneous catalysts.<sup>[7]</sup> Multiple functionalities like carboxyl, carbonyl, methyl, and methylene in LA ensures its facile participation for several organic transformations.<sup>[8]</sup>

LA, being one of the carbohydrates derived building block chemical identified by DOE,<sup>[9]</sup> is a promising biomass based chemical platform for industrial use through R&D. Recently, organic transformations of LA in presence of other biomass derived molecules to industrially valuable products (Scheme 1) are being pursued all over the world. Some prominent examples are: polymer precursors (ketals) through condensation of LA with glycerol,<sup>[10]</sup> diphenolic acid (a renewable plasticizer-alternative to bisphenol A) from LA reacting with phenol,<sup>[11]</sup> alkyl levulinates (fuel oxygenates) via esterification of LA with C1-C4 linear and/or branched alcohols,<sup>[12]</sup> and production of liquid alkanes (fuels) from LA with formic acid via intermediate of  $\gamma$ -valerolactone (Gvl). It is worth mentioning here that formic acid is the by-product in LA synthesis from C6-sugars that can act as a hydrogen source for the synthesis of Gvl, a key step in a bio-refinery.<sup>[13]</sup>



**Scheme 1.** Valuable products from catalytic transformations of LA with other biomass-based molecules

Moreover, LA in presence of furfural (hemicellulose-derived) undergoes aldol condensation using base catalysts to form an aldol adduct which is a precursor for polymer and fuel.<sup>[14]</sup> Li's research group reported lipase-catalyzed esterification of LA with HMF (cellulose-derived) in 2-methyltetrahydrofuran (2-MeTHF) medium, which formed HMF-levulinate that may be useful as fuel additive.<sup>[15]</sup> Furthermore, LA is used in catalysed ring opening of

[a] Sreedhar Gundekari, Kannan Srinivasan  
Inorganic Materials and Catalysis Division  
CSIR-Central Salt and Marine Chemicals Research Institute  
GB Marg, Bhavnagar - 364 002, India  
E-mail: [skannan@csmcri.res.in](mailto:skannan@csmcri.res.in); [kanhem1@yahoo.com](mailto:kanhem1@yahoo.com)

[b] Sreedhar Gundekari, Kannan Srinivasan  
Academy of Scientific and Innovative Research  
CSIR-Central Salt and Marine Chemicals Research Institute  
GB Marg, Bhavnagar - 364 002, India  
Supporting information for this article is given via a link at the end of the document.

## FULL PAPER

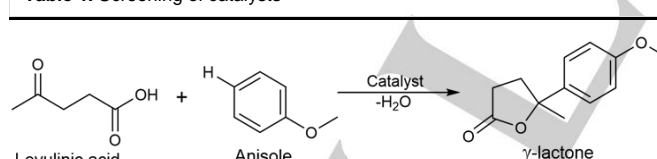
epoxidized methyl oleate (EMO) for the preparation of branched oleochemicals; in presence of LA, EMO formed two products (ketal and ester) by varying the reaction conditions.<sup>[16]</sup> The dehydrated product of LA such as angelica lactone (AL) reacts with another two AL and/or two 2-methylfuran in presence catalysts form C-C bonded alkylated furan and lactone products which are precursors for transportation fuels.<sup>[17]</sup> LA functionality is also reported for the reductive amination reaction for the preparation of pyrrolidones (industrial solvents) using amines under H<sub>2</sub>.<sup>[18]</sup>

Among the mentioned LA-based products; Gvl has been studied extensively for its preparation and applications. It can be prepared through hydrocyclization of LA under H<sub>2</sub> using metal supported catalysts, and we reported recently this conversion using *in situ* generated Ru catalyst via hydrous ruthenium oxide.<sup>[19]</sup> Gvl, a promising precursor for liquid alkanes, polymers and itself a greener solvent, is a member of the class of  $\gamma$ -lactones.<sup>[20]</sup>  $\gamma$ -lactone containing moieties are relevant in many areas like pharmaceutical, agrochemicals, polymers, and precursors to the production of furans, cyclopentenones and natural products.<sup>[21]</sup> In particular, certain aryl/methyl substituted  $\gamma$ -lactones have significant biological activity towards cytotoxicity (against cancer cells), anti-inflammatory ability and helps in increasing human growth hormone levels for enhancing the quality of life.<sup>[22]</sup> Currently, such arylated  $\gamma$ -valerolactones (Agvls) are prepared from petroleum-derived feedstock only. The approach to synthesize both existing & novel Agvls from biomass based chemicals is interesting and has been envisioned to have a significant impact on pharmaceutical research.

Continuing our interest in the synthesis and value addition of biomass-based chemicals, we report here an efficient transformation of biomass-based LA with aromatics to Agvls using recyclable H- $\beta$  zeolite catalyst under solvent-free conditions.

## Results and Discussion

**Table 1.** Screening of catalysts<sup>[a]</sup>



Entry	Catalyst	Conv. of LA <sup>[b]</sup> (%)	Yield of lactone <sup>[b]</sup> (%)	Sel. of lactone (%)
1	Blank	n.r	-	-
2	Na- $\beta$	22	20	91
3	Na-Y	n.r	-	-
4	Na-ZSM-5	n.r	-	-
5	H- $\beta$	27	25	92

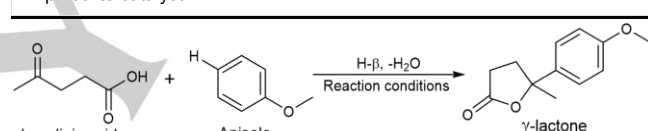
[a] LA: anisole molar ratio-1:1 (LA (1g; 8.6 mmol), anisole (8.6 mmol)), catalyst (20 wt% w.r.t LA), 120 °C, 6 h. [b] Theoretical conversion of LA and yield of Agvl (isolated using column chromatography). n.r.-No reaction.

Formation of arylated  $\gamma$ -valerolactones (Agvls) from LA with aromatics is an acid catalysed reaction. Thus, zeolites were

chosen for catalyst screening studies as their multifunctional characteristics such as highly crystalline, thermally stable, tunable acidity, reusability, and shape selectivity that are used in many organic transformations including in petrochemical industry.<sup>[23]</sup> Further, zeolites have been demonstrated for excellent activity for diverse catalytic transformation of biomass/biomass-derived compounds, and were also reported as good acidic supports.<sup>[24]</sup>

Screening of catalysts was performed with 20 wt% (w.r.t. LA) of different zeolitic materials using 1:1 molar ratio of LA to anisole (Table 1). Blank reaction (without catalyst) and among the zeolites screened, only  $\beta$ -zeolites namely Na- $\beta$  and H- $\beta$  were active towards the reaction, which showed 22 and 27% conversion of LA with excellent selectivity of 91 and 92% to para-substituted Agvl (Table 1, entries 2 and 5). The high activity of  $\beta$ -zeolite is probably due to unique pore topology and presence of local defects in their structures through octahedral extra-framework aluminium (AlO<sub>6</sub>) that generates Lewis acidic properties, which results in efficient conversion and product selectivity in several organic transformations, as reported in the literature.<sup>[25]</sup> Between Na and H- $\beta$  zeolite, the latter showed comparatively better activity and thus the reaction parameter variation studies were conducted further with this catalyst.

**Table 2.** Optimization studies for Agvl formation from LA with anisole using H- $\beta$  zeolite catalyst<sup>[a]</sup>



Entry	T. (°C)	Catalyst (wt % w.r.t LA)	Molar ratio	Solvent	Conv. of LA <sup>[b]</sup> (%)	Yield of lactone (%)
1	40	10	1:1	Neat	1-2	trace
2	80	10	1:1	Neat	4-5	trace
3	120	10	1:1	Neat	16	15
4	120	10	1:1	CH <sub>3</sub> -OH	80	n.o
5	120	10	1:1	DMSO	n.r	-
6	120	10	1:1	ACN	n.r	-
7	120	10	1:1	THF	n.r	-
8	120	10	1:1	CH	n.r	-
9	150	10	1:1	Neat	34	30
10	150	10	1:2	Neat	51	47
11	150	10	1:4	Neat	63	59
12	150	10	1:6	Neat	61	58
13	150	30	1:4	Neat	78	70
14 <sup>[d]</sup>	150	30	1:4	Neat	52	43
15 <sup>[e]</sup>	150	30	1:4	Neat	39	27
16 <sup>[f]</sup>	150	30	1:4	Neat	33	18
17	150	50	1:4	Neat	85	77
<b>18<sup>[c]</sup></b>	<b>150</b>	<b>50</b>	<b>1:4</b>	<b>Neat</b>	<b>90</b>	<b>82</b>
19 <sup>[g]</sup>	150	50	1:4	Neat	89	81

[a] LA (4.3 mmol, 500 mg), anisole (4.3-25 mmol (465.5-1793 mg)), H- $\beta$  (50-250 mg), solvent (2.5 ml), 6 h. [b] Theoretical conversion of LA and yield of Agvl (isolated using column chromatography). [c] 12 h. [d, e, f] Reaction with MeL, EtL, BuL respectively. [g] Reaction with isolated anisole (from product mixture). n.r.-No reaction, n.o.- Not observed, ACN-Acetonitrile, CH-Cyclohexane.

Generally, an increase in the reaction temperature increases the rate of the reaction, as this factor raises the average kinetic energy of the reactant molecules that leads to effective

## FULL PAPER

collision. By considering this fact, we varied reaction temperature which revealed that the reaction is critically dependent on the reaction temperature wherein the yield of  $\gamma$ -lactone gradually increased from 2% to 30% with an increase in the temperature from 40 to 150 °C under solvent-free conditions with 1:1 molar ratio of reactants (Table 2, entries 1-3 and 9). In presence of either polar (both protic and aprotic) or non-polar solvents, under similar conditions, the catalytic activity for  $\gamma$ -lactone formation was hampered; in the case of methanol as solvent, we observed methyl levulinate with 80% conversion and 100% selectivity while other solvents such as dimethyl sulfoxide, acetonitrile, tetrahydrofuran, and cyclohexane did not show any conversion of LA (Table 2, entries 4-8). Though the reasons are unclear, the dielectric/polarity of the medium and the influence of solvent on the acidic sites are probably the reasons for poorer interaction between the reactant with zeolite, and in turn on the activity.

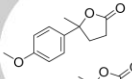
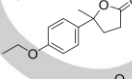
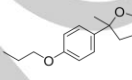
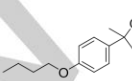
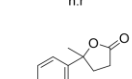
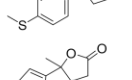
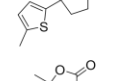
On increasing the anisole concentration from 1 to 6 equivalent w.r.t LA, we observed an increase in the conversion of LA and with this yield of  $\gamma$ -lactone also increased up to 59% for 4 equivalent anisole (sufficient for optimal interaction) and stabilizes even on a further increase (6 equivalent) in the amount of anisole (Table 2, entries 9-12). Thus, we chose 1:4 (LA: anisole) equivalent for further experiments. It is worth mentioning here that during the reaction, the keto carbon of LA gets partial positive charge (see mechanism); and to neutralize sufficient to excess of aromatic molecules are needed.

Reaction conducted using LA esters such as methyl levulinate (MeL), ethyl levulinate (EtL) and butyl levulinate (BuL) showed lesser conversion towards the formation of  $\gamma$ -lactone compared to that of LA (Table 2, entry 14-16). Mechanistically when using LA as reactant, the cyclization step is an intramolecular esterification while for levulinic ester cyclization involves intramolecular trans-esterification. Compared to trans-esterification, esterification is more favourable, and thus LA showed higher conversion than levulinic esters and this is in accordance with our earlier report with evidence on cyclization of LA and its esters for Gvl production.<sup>[19b, 26]</sup> Furthermore, an increase in the chain length (from MeL to BuL) influences the diffusion of the molecules (besides subtle increase in the molecular hydrophobicity) affects the approach of molecule to the active acidic centres of the zeolite and thus could be reason for the reduced activity. Interestingly, in all three LA esters, nearly 3-5% of LA as side product was formed probably due to acidic hydrolysis of LA esters using H<sub>2</sub>O formed during the reaction. From the above discussion, we concluded that compared to LA esters, the LA is an effective reactant for the formation of  $\gamma$ -lactone, and thus used as reactant for further experiments.

Further, we varied the catalyst amount (10 - 50 wt% w.r.t LA), wherein a maximum of 77%  $\gamma$ -lactone yield was obtained at 50 wt% of catalyst (Table 2, entries 13 and 17). An increase in the wt% of catalyst enhances the number of acidic sites and thereby increases interaction of LA with the active centres and in turn resulting in higher conversion of reactants towards the formation  $\gamma$ -lactone. Reaction time variation studies showed a slight increase in the product yield after 12 h reaction (Table 2, entries 17 and 18). From above parametric studies, the best yield of  $\gamma$ -lactone was obtained with 4:1 molar ratio of anisole to LA under solvent-free conditions at 150 °C using 50 wt% catalyst loading in 12 h (Table 2, entry 18). The excess equivalent amount of anisole to the reaction generates waste while conducting bulk experiments. Thus, to avoid this drawback, after the reaction the

unreacted/excess amount of anisole was recovered while separation of product ( $\gamma$ -lactone) using column chromatography, and the recovered anisole is re-used for the reaction that showed similar conversion of LA (89%) and yield of  $\gamma$ -lactone (81%) under optimised reaction conditions (Table 2, entries 18 and 19).

**Table 3.** Synthesis of Agvls from LA with various aromatics using H- $\beta$  zeolite catalyst<sup>[a]</sup>

Entry	Aromatic	$\gamma$ -lactone	Conv. (%)	Yield (%)	Sel. (%)
1 <sup>[b]</sup>			90	82	91
2 <sup>[b]</sup>			70	60	86
3 <sup>[b]</sup>			74	63	85
4 <sup>[b]</sup>			78	67	86
5 <sup>[c]</sup>		n.r	-	-	-
6 <sup>[c]</sup>		n.r	-	-	-
7 <sup>[b]</sup>			48	40	83
8 <sup>[b, d]</sup>			93	84	90
9 <sup>[c, e]</sup>			96	77	80
10 <sup>[c]</sup>		n.o	-	-	-
11 <sup>[c]</sup>		n.o	-	-	-

[a] LA to aromatic molar ratio is 1:4 (LA (4.3 mmol), aromatics (17.2 mmol)), H- $\beta$  (50 wt% w.r.t. LA), 150 °C for 12 h. [b] Theoretical conversion of LA and yield of Agvls (isolated using column chromatography). [c] GC-MS conversion and yield. [d] 110 °C, [e] 85 °C. n.r-No reaction, n.o-Not observed.

The substrate scope for the synthesis of  $\gamma$ -lactones were extended with molecules having linear alkoxy benzenes (ethoxy to butoxy benzenes). Increasing the alkyl chain length slightly increased the conversion of LA with the retention of selectivity of para-substituted  $\gamma$ -lactones (Table 3, entries 2-4). We further strived to extend the reactant scope using simple aromatic hydrocarbon cumene, but in this case, no reaction was observed. This could be due to the fact that the aromatic ring in cumene is not electronically rich enough to participate in the nucleophilic attack on the carbonyl carbon of LA. The increase in the ring electron density is thus provided by the lone pair of electron present on the heteroatom in the substrates with electron donating substituents. Thus, the absence of such electron

## FULL PAPER

donating substituent in cumene precludes the formation of  $\gamma$ -lactone (Table 3, entry 5).

The above explanation was further supported by the observation of 48% conversion of LA while using thioanisole as aromatic moiety, that showed 83% selectivity of para isomeric  $\gamma$ -lactone (Table 3, entry 7). Thus, the lone pair of electrons on a heteroatom containing substituent on the benzene ring increases the electron density on the para position and facilitates the nucleophilic attack on the carbonyl carbon of LA. Further, we explored the synthetic protocol by using sulphur containing five-membered heterocycles, chosen owing to higher resonance energy compared to oxygen and nitrogen-containing heterocycles. 2-methylthiophene and thiophene showed excellent selectivity towards the  $\gamma$ -lactone formation (90% and 80%) with 93% and 96% conversion of LA (Table 3, entry 8 and 9).

The nitrogen and phosphorous containing aromatics did not show  $\gamma$ -lactone formation under the reaction conditions studied over H- $\beta$  catalyst. The N,N-Dimethyl aniline formed dimerised product (tetramethyl-[1,1'-biphenyl]-diamine) as confirmed by GC-MS analysis while triphenylphosphine resulted in the formation of triphenylphosphine oxide as a product (Table 3, entry 10 and 11). Para isomer was obtained as the exclusive product for six-membered ring containing substrates, suggesting a product shape selectivity exhibited by the catalyst. The para isomers being less bulky can easily diffuse in the zeolitic pores compared to ortho- and meta- isomers. To corroborate, we conducted a reaction using 1-ethoxy-4-methoxybenzene in which the para position of the methoxy is blocked. The absence of  $\gamma$ -lactone supports the regioselectivity towards para isomer under our experimental conditions (Table 3, entry 6).

Assessment of recyclability of the catalyst is beneficial for industrial applications, as it helps in reducing the cost of the process. After the reaction, the colour of the catalyst (H- $\beta$ ) changed from white to red. The used catalyst was washed with DCM and dried at 100 °C for 12 h. The oven dried catalyst (termed UH- $\beta$ ) was reused under similar reaction conditions that showed a decrease in the yield of  $\gamma$ -lactone up to 40% without any compromise in selectivity (Figure 1, cycle 2). The decrease in the catalytic activity is due to adherence of organic carbon that formed during the reaction which probably blocked the acidic sites of the catalyst, and in turn, decreased the catalytic activity. The detailed study of organic carbon deposition in used  $\beta$ -zeolite is discussed in the catalyst characterization section.

The used catalyst (UH- $\beta$ ) was calcined at 550 °C for 3 h to remove the adhered organic carbon under air. After calcination, the catalyst colour changed back to white from red (UH- $\beta$ ) and is henceforth referred to as UH- $\beta$ C. The UH- $\beta$ C showed similar reactivity for the synthesis of  $\gamma$ -lactone as that of fresh H- $\beta$  catalyst, resulting in similar yield and selectivity of the product (Figure 1, cycle 3). However, the product yield/LA conversion marginally decreased upon recycling (Figure 1, cycle 4 and 5). The decrease in the activity is presumably due to the depletion of Brönsted acidic sites (H<sup>+</sup>) through their dissolution in water, a by-product formed in the reaction. The calcined catalyst was treated with dilute mineral acid followed by washing (with water) and drying at 120 °C for 3 h. The regenerated catalyst (UH- $\beta$ C) after acid

treatment showed similar catalytic activity as that of fresh catalyst for several further cycles (Figure 1, cycle 6-9).

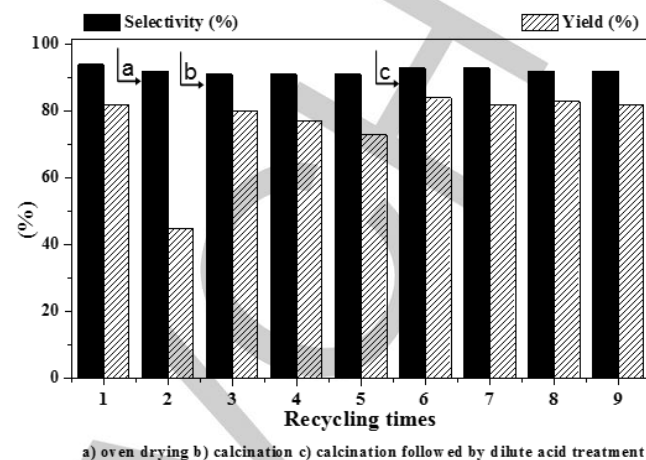


Figure 1. Recyclable studies of H- $\beta$  zeolite

LA to aromatic molar ratio is 1:4 (LA (4.3 mmol, 0.5 g), anisole (17.2 mmol, 1.86 g)), H- $\beta$  (50 wt % w.r.t. LA), 150 °C for 6 h. Isolated yield of the product has been considered here.

#### Catalyst characterization



Figure 2. Physical appearance of various stages of  $\beta$ -zeolites

The presence of organic carbon in the UH- $\beta$  and its removal in UH- $\beta$ C on calcination were characterized using multiple analytical tools like PXRD, FT-IR, CHNS, TOC, CP MAS-NMR (<sup>13</sup>C, and <sup>27</sup>Al), SEM, textural measurements (specific surface area and pore volume), TGA, TPD and UV-visible spectroscopy. The physical appearance of different stages of  $\beta$ -zeolite (H- $\beta$ , UH- $\beta$ , and UH- $\beta$ C) are given in Figure 2.

The PXRD of the H- $\beta$  matched well with the precursor Na- $\beta$  suggest that the crystalline structure of zeolite did not change upon its conversion. Further, the crystallinity of the catalyst was not affected even after several catalytic cycles with intermittent calcination Figure 3.

The FT-IR of UH- $\beta$  showed additional bands when compared with that of fresh H- $\beta$  zeolite in the region 1500-2000

## FULL PAPER

cm<sup>-1</sup> which disappeared upon calcination (UH-βC) (see Figure 1 in the ESI). In other words, FT-IR conforms the deposition of organic carbon moiety in UH-β zeolite presumably having carbonyl/carboxy functional groups. The NH<sub>3</sub>-TPD analysis showed a decrease in the total amount of NH<sub>3</sub> adsorbed from 0.70 mmol/g for H-β to 0.58 mmol/g for UH-β, further supporting the blockage of acidic sites in UH-β catalyst due to the presence of organic carbon. The regenerated catalyst (UH-βC) showed restoration in acidity (0.69 mmol/g NH<sub>3</sub>) (see Figure 2 in the ESI).

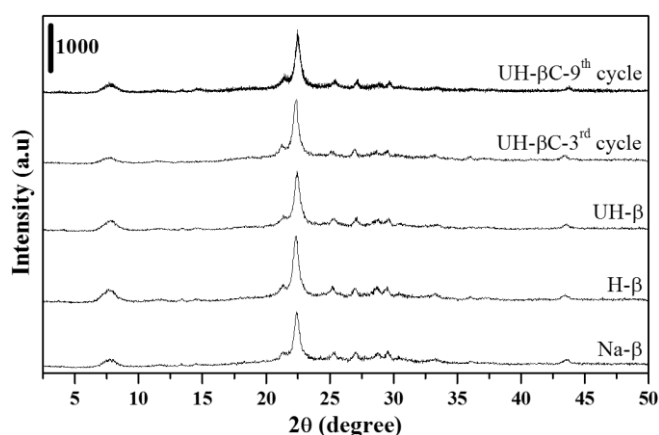


Figure 3. PXRD of β-zeolite catalysts

The Py-FTIR (Figure 4), showed bands at 1445 and 1595 cm<sup>-1</sup> for fresh H-β catalyst indicating the presence of Lewis-acidic sites,<sup>[27]</sup> that are responsible for facilitating this reaction. These bands, however, disappeared for the used catalyst (UH-β) and reappeared for the calcined catalyst (UH-βC) augmenting the relationship between Lewis acidity and catalytic activity. Thus, the removal of deposited organic carbon moieties that adhere over Lewis acidic sites upon calcination restores the acidic sites. In other words, the organic carbon moieties formed in the course of the reaction blocked the Lewis acidic sites of the UH-β zeolite which could be restored by removing them by calcination. In so forth, the absence of these sites is the likely reason for the poor activity exhibited by Na-Y and Na-ZSM-5 (Figure 4a and b), though their textural properties were not significantly different from Na/H-β (Table 1 in the ESI).

Furthermore, Py-FTIR of both Na/H-β zeolite showed bands at 1545 cm<sup>-1</sup> ascribed to Brönsted acidic sites (probably due to incomplete exchange) and the band at 1490 cm<sup>-1</sup> attributed to the mixture of both acidic sites (Brönsted and Lewis) (Figure 4).<sup>[18]</sup> The slightly higher activity of H-β over Na-β is probably due to cooperative mechanism of both sites (see mechanism). Incidentally, for UH-β, though had Brönsted acidic sites (Figure 4 e), it was not enough to drive the reaction further necessitating the requirement of Lewis acidic sites.

The organic carbon deposition in the used catalyst (UH-β) has also been confirmed by the increase in carbon content measured through CHNS and TOC (total organic carbon). The CHNS analysis (Table 4) of catalysts showed an increase to 9% carbon for UH-β from 0.8% for H-β. This value decreased to ~0.5% for UH-βC. Such variation in the carbon content has also

been supported by TOC measurements (Table 4). Thus, the removal of organic carbon moieties upon calcination causes the calcined catalyst to behave similar to that of the fresh catalyst.

Table 4. CHNS and TOC analysis of β-zeolite catalysts

Element	CHNS			TOC		
	H-β	UH-β	UH-βC	H-β	UH-β	UH-βC
Carbon	0.79	8.89	0.26	-	9.0	-

TGA analysis of the catalysts (Figure 5a) showed 10% weight loss for fresh H-β in the temperature range 50-150 °C, due to desorption of physisorbed H<sub>2</sub>O molecules. In addition to this weight loss, UH-β showed weight loss around 160-320 °C and 350-620 °C which corresponds to the removal of deposited organic carbon moiety in the catalyst, amounting to ~20% loss in weight. The weight loss mechanism of carbon under oxygen environment is common for a typical organic compound, wherein initially, the organic carbon material adsorbs oxygen with a gain in weight while a further increase in the temperature leads to oxidation with an evolution of CO<sub>2</sub>/CO and thereby reduces the weight.<sup>[28]</sup> The calcined catalyst (UH-βC) showed weight loss (10%) similar like fresh H-β at the temperature range 50-150 °C, as the organic carbon has already been removed by prior calcination.

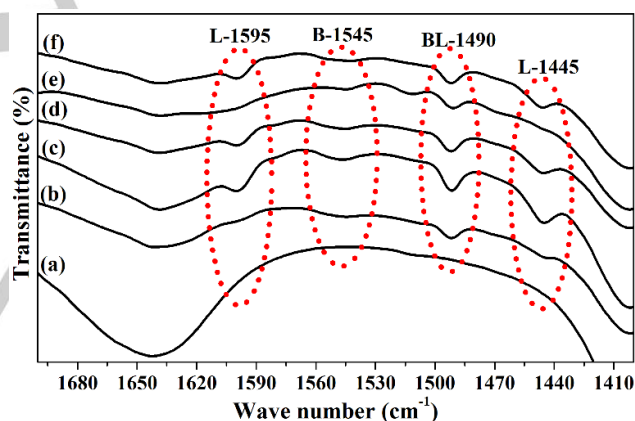


Figure 4. Py-FTIR spectra of β-zeolite catalysts; (a) Na-Y, (b) Na-ZSM-5, (c) Na-β, (d) H-β, (e) UH-β, and (f) UH-βC

The UV-visible spectra of fresh H-β catalyst did not show any transitions in the entire wavelength range studied suggest the obvious absence of UV active groups in β-zeolite. However, in the case of used H-β catalyst (UH-β) three major transitions were observed around 630, 515 and 390 nm corroborating the presence of deposited organic carbon in the zeolite (Figure 5b). From the above observation, one may conclude the presence of UV active functional groups in such deposited organic moieties corroborating FT-IR results. The reactivated catalyst (UH-βC), as anticipated, did not show any transition in the UV-visible spectrum similar to that of fresh catalyst (H-β). These results also clearly provide conclusive support for the removal of deposited organic carbon by calcination.

## FULL PAPER

The scanning electron microscopic (SEM) analysis of H- $\beta$ , UH- $\beta$  and UH- $\beta$ C are shown in Figure 6. The catalyst (H- $\beta$ ) depicted spherical morphology with regular arrangement. On the contrary, UH- $\beta$  catalyst showed irregular morphology with thread and rod like structures of organic carbon moieties. In view of this, LA and anisole molecules have diffusion limitation towards the active acidic sites of the zeolite and thus causes a decrease in the catalytic activity. However, on removal of the organic carbon for the calcined catalyst (UH- $\beta$ C), the rods and threads were absent and the morphology obtained was also similar to that of the fresh catalyst (H- $\beta$ ), the initial activity was restored.

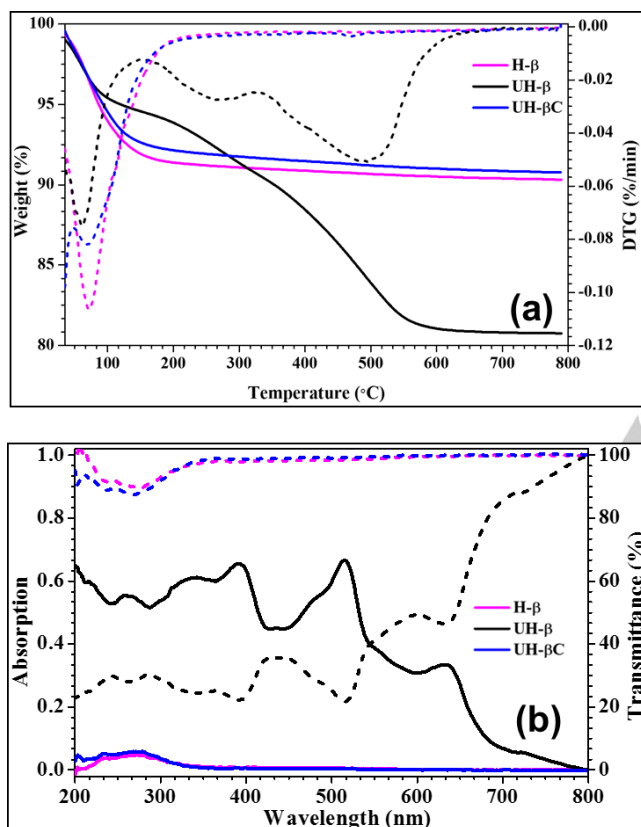


Figure 5. TGA (a) and UV-visible spectra (b) of  $\beta$ -zeolite catalysts

The SEM-energy dispersive X-ray elemental analysis (SEM-EDX) of the catalysts were recorded and shown in Figure 3 in the ESI. All samples were analysed in a specimen stub that had 11% carbon. The EDX of UH- $\beta$  showed 22% carbon, in other words, suggest 11% of carbon in UH- $\beta$ , whose value is closer to the TOC and CHNS measurements. Furthermore, the EDX-maps of UH- $\beta$  zeolite revealed the location of organic carbon moiety in zeolite matrix (see Figure 4 in the ESI).

The textural properties of zeolites (H- $\beta$ , UH- $\beta$ , and UH- $\beta$ C) are mentioned in Table 1 in the ESI. The BET surface area of fresh H- $\beta$  was found to be 501 m<sup>2</sup>/g with a pore volume of 0.32 cm<sup>3</sup>/g which decreased sharply for the used catalyst (UH- $\beta$ ) to 326 m<sup>2</sup>/g and 0.27 cm<sup>3</sup>/g. The organic carbon moiety have blocked the pores and consequently, a decrease in the pore volume/specific surface area of the zeolite was noted. After

calcination, a restoration of both surface area and pore volume was observed for UH- $\beta$ C: surface area (535 m<sup>2</sup>/g) and pore volume (0.33 cm<sup>3</sup>/g).

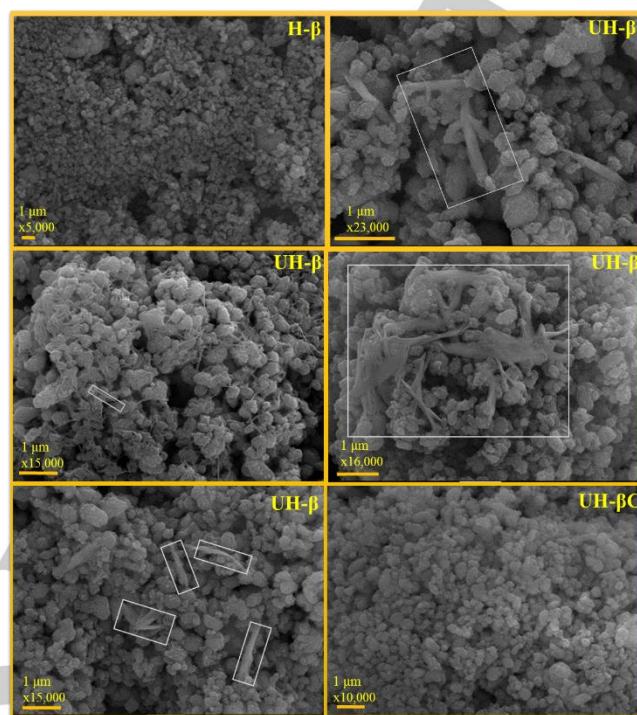


Figure 6. SEM images of zeolites

Solid state NMR is an important tool to predict the structural changes in zeolite as a consequence of the catalytic reactions. The <sup>13</sup>C, and <sup>27</sup>Al CP-MAS NMR of all three catalysts (H- $\beta$ , UH- $\beta$ , and UH- $\beta$ C) were studied. <sup>13</sup>C CP-MAS NMR has earlier been deployed for the identification of carbon deposition in the zeolites like Y,  $\beta$ , and ZSM-5.<sup>[28e, 29]</sup> Absence of peaks in <sup>13</sup>C CP-MAS NMR spectrum of fresh H- $\beta$  zeolite supported the absence of carbon containing moieties in the catalyst. However, UH- $\beta$  catalyst showed peaks at 29, 50, 87, 114, and 181  $\delta$  ppm. The 29 and 50  $\delta$  ppm peaks may be of saturated alkyl carbon, the 87 and 114  $\delta$  ppm peaks correspond to alcohol/ether/alkyne carbon. The 181  $\delta$  ppm supports the presence of carboxylic acid group. Thus, the deposited organic carbon could probably be alcoholic/carboxylic acid based material. The reactivated catalyst (UH- $\beta$ C) also did not show any peaks in the <sup>13</sup>C CP-MAS NMR (Figure 7a).

The <sup>27</sup>Al CP-MAS NMR of catalysts given in Figure 7b, showed primarily two peaks. The major peak approximately in the range of 54-55  $\delta$  ppm attributed to 4-coordinated tetrahedral framework of aluminium (AlO<sub>4</sub>) species and minor peak in range of 0.15-0.62  $\delta$  ppm corresponding to octahedral extra-framework aluminium (AlO<sub>6</sub>).<sup>[28e, 30]</sup> On comparing H- $\beta$  and UH- $\beta$ C, the octahedral aluminium peak of UH- $\beta$  zeolite showed larger broadening indicating a structural distortion in the AlO<sub>6</sub> framework of the zeolite probably due to interaction of deposited organic carbon moiety. The AlO<sub>6</sub> is responsible for the Lewis acidic sites

## FULL PAPER

in the  $\beta$ -zeolite and thus relevant to the reaction described in this work. However, in the case of used zeolite (UH- $\beta$ ), the formed organic moiety blocked/modified the extra-framework Lewis acidic sites of  $\text{AlO}_6$ , and thus resulting in the observed decline in the catalytic activity. The reactivated catalyst (UH- $\beta$ C) obtained upon calcination showed a sharp peak at 0.6  $\delta$  ppm similar to the fresh  $\beta$ -zeolite suggests the restoration of the structure of the catalyst.

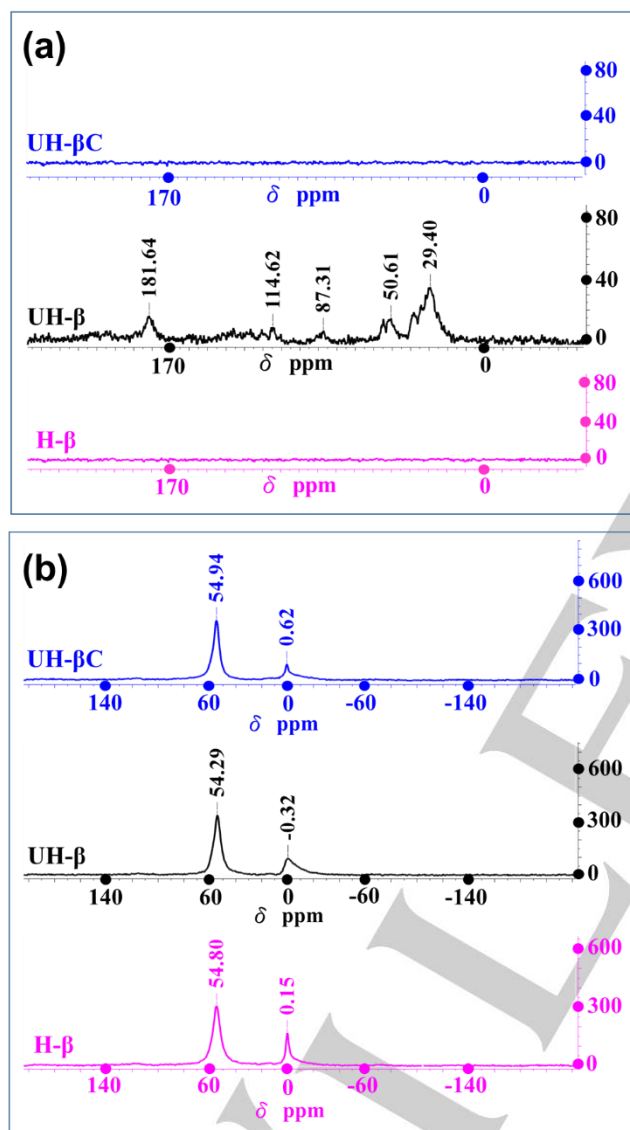


**Figure 7.** CP-MAS NMR of  $\beta$ -zeolite catalysts; (a)  $^{13}\text{C}$  CP-MAS NMR (b)  $^{27}\text{Al}$  CP-MAS NMR

A scalability study for the synthesis of  $\gamma$ -lactone was carried out at 10 g of LA with anisole. An increase in the yield of  $\gamma$ -lactone was observed with an increase in time. After 6, 12, 18 and 24 h; 38, 62, 80 and 90% yield of para substituted  $\gamma$ -lactone was obtained with 95, 94, 92 and 90% selectivity respectively (Figure 8).

A probable mechanism has been proposed for the formation of arylated  $\gamma$ -lactones (Figure 9). First, the lone pairs of keto group of LA interact with the Lewis-acidic sites of aluminium that are present due to the local defects in zeolitic framework.<sup>[25, 31]</sup> The development of a partial positive charge on the keto carbon initiates a nucleophilic attack via the electron rich para position of anisole and/or other active substrates resulting in formation of  $\gamma$ -hydroxy pentatonic acid intermediate. This being unstable undergoes ring cyclization (intra-molecular esterification) to  $\gamma$ -lactone with the removal of water.<sup>[32]</sup> The slightly higher activity of H- $\beta$  zeolite compared to Na- $\beta$  is probably due to the presence of protons (Brönsted acidic) on the surface of H- $\beta$  zeolite that facilitates the reaction.

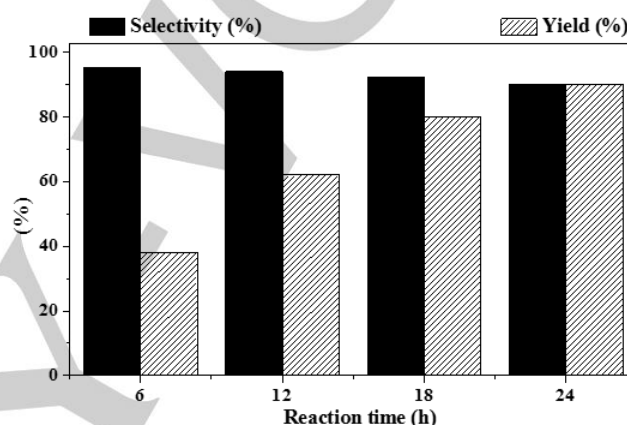


**Figure 8.** Scale up studies ( $\gamma$ -lactone yield and selectivity vs. time (h)). LA to aromatic molar ratio is 1:4 (LA (86 mmol, 10 g), anisole (344.8 mmol, 37.2 g)), H- $\beta$  (50 wt% with respect to LA), 150 °C. Yields are determined by gas chromatography.

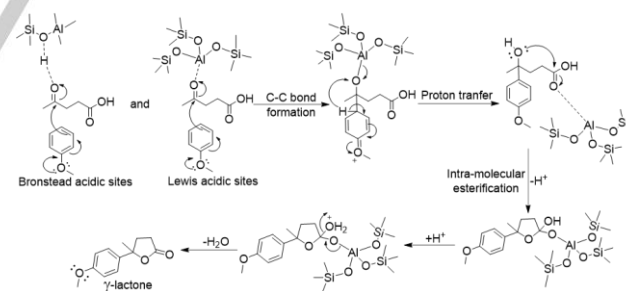


**Figure 9.**  $\beta$ -zeolite catalysed mechanistic pathway for Agvl formation

The obtained Agvl were structurally confirmed by  $^1\text{H}$  and  $^{13}\text{C}$  NMR spectroscopy, a representative example of  $^1\text{H}$  NMR of Agvl (anisole aromatic product: 5-(4-methoxyphenyl)-5-methylidihydrofuran-2(3H)-one) is shown in Figure 10. The presence of two doublets in the aromatic region (7.3-7.29 and 6.9-6.88  $\delta$  ppm) confirmed selective para substitution. The  $^{13}\text{C}$  NMR showed a peak at 86.9  $\delta$  ppm evince chemo- and regioselective formation of Agvl's contrary to the formation of 1,4-diketones (which would show peaks around 200 and 205  $\delta$  ppm for keto groups which were absent in our  $^{13}\text{C}$  NMR) by Friedel-Crafts acylation (Figure 5 in the ESI). The other six membered aromatic

## FULL PAPER

products were also showed similar  $^1\text{H}$  and  $^{13}\text{C}$  NMR profile like the above mentioned anisole product. The  $^1\text{H}$  and  $^{13}\text{C}$  NMR data of the synthesized Agvls samples were re-recorded after 6 months of time to ascertain their bench stability. No noticeable

change in the spectral data was observed asserting that the isolated products (Agvls) were stable for prolonged periods. The spectral analysis of corresponding products are depicted in Figure 6A-L in the ESI.

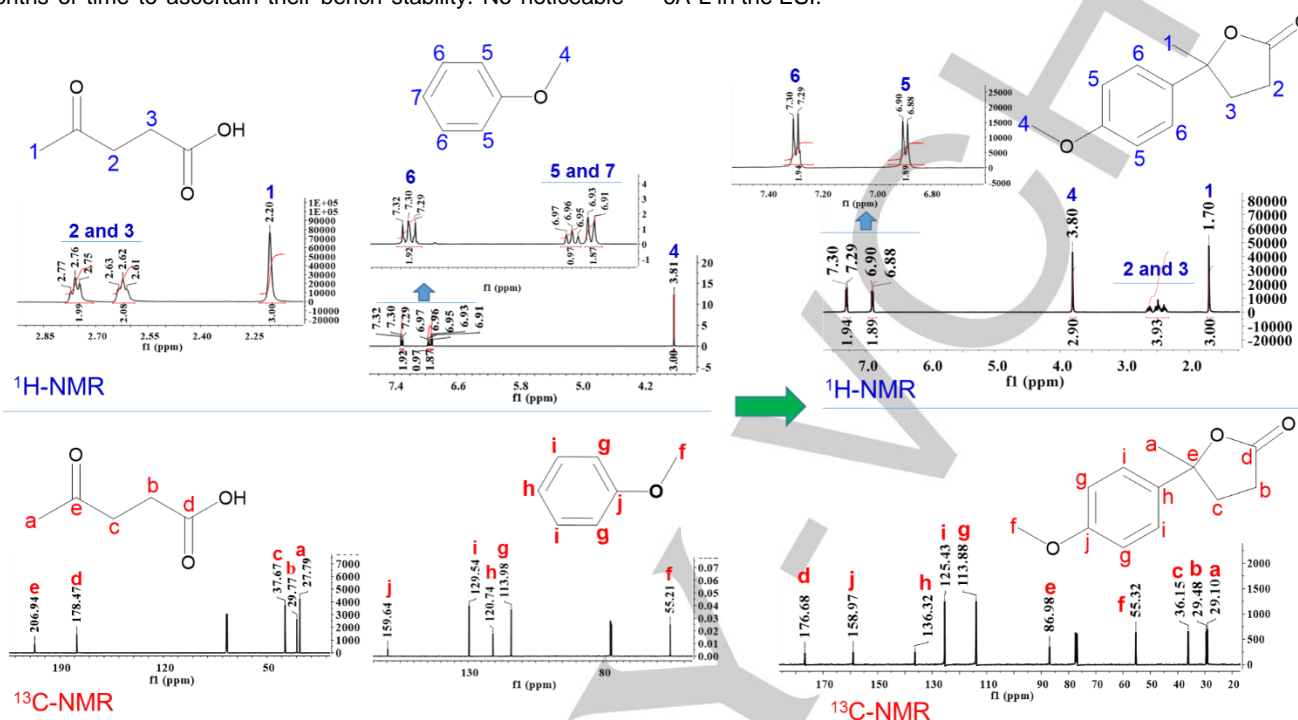


Figure 10.  $^1\text{H}$  and  $^{13}\text{C}$  NMR representation for formation of  $\gamma$ -lactone formation from LA with anisole

## Conclusions

In summary, herein we report a green synthetic protocol for the synthesis of arylated  $\gamma$ -valerolactones (Agvls) from LA and oxygen or sulphur-containing electron rich aromatics using recyclable  $\beta$ -zeolite as catalyst. The reaction is highly chemo- and regioselective as evinced by  $^1\text{H}$  and  $^{13}\text{C}$  NMR. Reaction scope studies with various aromatic compounds including five membered heterocyclics unravelled the structural requirements necessary in enabling this reaction. The reaction was successfully scaled to 10 g that yielded 90% of the para isomer in 24 h. The synthesized Agvls are stable in air for several months. The formation of organic carbonaceous moiety during the reaction, responsible for catalyst deactivation, was ascertained through several physicochemical, spectroscopic and microscopic techniques, whose removal by calcination regenerated the activity of the catalyst. Sustainable preparation of Agvls demonstrated in the present work is expected to spur interest among biomass researchers and process chemists in rendering new/novel products.

## Experimental Section

### Materials and methods

Levulinic acid (98%), methyl levulinate ( $\geq 98\%$ ), ethyl levulinate (99%), and butyl levulinate (98%) were purchased from Sigma-Aldrich. Some of the aromatics and solvents used such as thiophene, anisole, cumene, N,N-Dimethyl aniline, triphenylphosphine, methanol, and dichloromethane (DCM) were purchased from local vendors in India. Different zeolites used (Table 1) were purchased from Zeochem, Switzerland. H-form of zeolite and alkoxy benzenes except anisole were prepared using the reported procedure.<sup>[33]</sup>

### Catalytic reaction

The desired aromatic compound (17.27 mmol, 4 equiv.), LA (4.31 mmol, 1 equiv.), and H- $\beta$  (250 mg, 50 wt% with respect to LA) were stirred at 150  $^\circ\text{C}$  for 12 h at 600 rpm. After the completion of the reaction, the reaction mixture was diluted with DCM under stirring for 30 min. at room temperature. The mixture was then centrifuged to collect the supernatant liquid and the catalyst was separated. The collected catalyst was stirred with DCM and centrifuged. The supernatant was dried over anhydrous  $\text{Na}_2\text{SO}_4$  and filtered. The reaction progress was monitored with thin-layer chromatography and the product mixture of  $\gamma$ -lactone was purified by column chromatography on silica gel (100-200 mesh) with

## FULL PAPER

ethyl acetate/hexane as the mobile phase. The isolated products were characterised by  $^1\text{H}$  &  $^{13}\text{C}$  NMR spectroscopy ( $\text{CDCl}_3$  solvent, Bruker, 500 MHz). In the case of thiophene, N,N-dimethyl aniline and triphenylphosphine as reactants, the reaction products were analysed using GC-MS. The reaction, analysis, and separation were done in duplicate and the error in the measurements were  $\pm 2\%$ .

### Catalyst characterization

PXRD measurement was carried out in a Philips X'Pert MPD system using  $\text{Cu K}\alpha$  radiation ( $\lambda=1.5406 \text{ \AA}$ ). The operating voltage and current were 40 kV and 30 mA, respectively. A step size of  $0.04^\circ$  with a step time of 2 seconds was used for data collection. The data were processed using the Philips X'Pert (version 2.2e) software. Identification of the crystalline phases was made by comparison with the JCPDS files.

Fourier transformed-infrared (FT-IR) spectra between 400 and  $4000 \text{ cm}^{-1}$  with an accumulation of 20 scans and  $4 \text{ cm}^{-1}$  resolution were recorded in a Perkin-Elmer, GX-FTIR instrument, using KBr pellets. The acidity of the zeolites (Na-Y, Na-ZSM-5, Na- $\beta$ , H- $\beta$ , UH- $\beta$ , and UH- $\beta\text{C}$ ) were analysed through pyridine adsorption and monitored using Fourier-transformed infra-red (Py-FTIR) spectroscopic technique. For py-FTIR analysis, the samples were initially oven-dried at  $100^\circ\text{C}$  for 3 h. To the oven dried sample (50 mg), 0.1 ml of pyridine was admixed directly. To remove the physisorbed pyridine present in the sample, the samples were dried in oven at  $120^\circ\text{C}$  for 1 h. The samples were cooled to room temperature and the spectra were recorded with a nominal resolution of  $4 \text{ cm}^{-1}$  in the spectral range of  $400\text{-}4000 \text{ cm}^{-1}$  using a KBr background and 15 scans were accumulated for each spectrum.

Specific surface area and pore size analysis of the samples were measured by nitrogen adsorption at  $-196^\circ\text{C}$  using a sorptometer (ASAP-2020, Micromeritics). The samples were degassed under vacuum at  $300^\circ\text{C}$  for 4 h prior to measurements in order to expel the physisorbed water molecules. The BET specific surface area was calculated by using the standard Brunauer, Emmett and Teller (BET) method on the basis of adsorption data. Pore volume and micropore area were also determined.

The electron microscopic study has been done with scanning electron microscope (JEOL series JSM-7100F) equipped with Oxford instruments energy dispersive X-ray spectrometer (EDX) facility. The samples were coated with gold using sputter coating before analysis to avoid charging effects during recording. Analyses were carried out with an accelerating voltage of 15 kV and a working distance of 10 mm, with magnification values in-between  $5000\times$  to  $30,000\times$ .

The acidity in  $\beta$ -zeolites (H- $\beta$ , UH- $\beta$ , and UH- $\beta\text{C}$ ) were analysed by  $\text{NH}_3$ -TPD desorption on a Micromeritics Autochem 2920 instrument. Initially, the samples were activated at  $150^\circ\text{C}$  under a helium flow to removal of physisorbed  $\text{H}_2\text{O}$  molecules and passed the ammonia gas at  $50^\circ\text{C}$  temperature. After,  $\text{NH}_3$  get observed in zeolites, the temperature was raised from  $50$  to  $500^\circ\text{C}$  with heating rate of  $10^\circ\text{C min}^{-1}$  and calculated desorbed  $\text{NH}_3$  in each sample.

Thermogravimetric analysis (TGA) was carried out in Mettler TGA/SDTA 851<sup>e</sup> and the data were processed using Star<sup>e</sup> software, in flowing oxygen and at a heating rate of  $10^\circ\text{C/min}$ .

The elemental analysis was carried out using Elementar, Vario Micro Cube CHNS analyser with combustion range  $1150^\circ\text{C}$  in presence of He as the carrier gas. The gases from the degraded samples were confirmed by using ADS resin column with TCD detector.

The total organic carbon (TOC) present in the catalysts (H- $\beta$ , UH- $\beta$ , and UH- $\beta\text{C}$ ) was measured by using Elementar instrument, Germany with soil Boden-Standard (Art-No: 35.00-0156). The sample reactor was maintained at  $800^\circ\text{C}$  the  $\text{CO}_2$  was detected and measured by using NDIR detector.

Solid-state NMR spectra were acquired on Bruker Avance II 500 MHz spectrometer equipped with a double-resonance CP-MAS probe. The  $^{27}\text{Al}$  MAS spectra were recorded at a spinning frequency of 8 KHz with 1024 scans using  $\text{AlCl}_3\cdot 6\text{H}_2\text{O}$  as reference and chemical shift range between 200 to  $-220 \delta$  ppm. The  $^{13}\text{C}$  MAS spectra were recorded at a spinning frequency of 8 KHz with 2048 scans using Tetramethylsilane (TMS) as reference in the chemical shift range between 250 to  $-50 \delta$  ppm.

The absorbance and transmittance were recorded using Shimadzu UV-2500 spectrophotometer, Japan.

### Abbreviations

Short form	Abbreviations
LA	Levulinic acid
Gvl	$\gamma$ -valerolactone
Agvls	Arylated $\gamma$ -valerolactones
MeL	Methyl levulinate
EtL	Ethyl levulinate
BuL	Butyl levulinate
DCM	Dichloromethane
UH- $\beta$	Used H- $\beta$ zeolite
UH- $\beta\text{C}$	Used H- $\beta$ zeolite calcined at $550^\circ\text{C}$ for 3 h

### Acknowledgements

CSIR-CSMCRI Article No. 075/2017. S.G. thanks CSIR, New Delhi, for a Senior Research Fellowship. The authors thank CSIR, New Delhi for financial support under the projects OLP-0031, CSC-0123, and MLP-0028. The authors thank Analytical Division & Centralized Instrumental Facilities of this institute for analytical support. The authors thank Dr. Joyee Mitra and Dr. Churchill A. Antonyraj for proof correction of the manuscript.

### Conflicts of interest

The authors declare no conflict of interest.

**Keywords:** Levulinic acid • arylated  $\gamma$ -valerolactones •  $\beta$ -zeolite • chemo- and regioselectivity • catalyst deactivation

## FULL PAPER

- [1] a) J. H. Clark, F. E. I. Deswarte, in *Introduction to Chemicals from Biomass* (Eds.: J. H. Clark, F. E. I. Deswarte), John Wiley & Sons, Ltd. **2008**, pp. 1-20; b) D. B. Turley, in *Introduction to Chemicals from Biomass* (Eds.: J. H. Clark, F. E. I. Deswarte), John Wiley & Sons, Ltd. **2008**, pp. 21-46.
- [2] a) F. H. Isikgor, C. R. Becer, *Polym. Chem.* **2015**, *6*, 4497-4559; b) H. L. Wang, Y. Q. Pu, A. Ragauskas, B. Yang, *Bioresour. Technol.* **2019**, *271*, 449-461.
- [3] a) P. Gallezot, *Chem. Soc. Rev.* **2012**, *41*, 1538-1558; b) G. Fiorentino, M. Ripa, S. Ulgiati, *Biofuels, Bioprod. Biorefin.* **2017**, *11*, 195-214.
- [4] a) A. Corma, S. Iborra, A. Velty, *Chem. Rev.* **2007**, *107*, 2411-2502; b) V. D. M. Patel, B. Husing, L. Overbeek, F. Terragni, E. Recchia, in *Medium and Long-term Opportunities and Risks of the Biotechnology production of Bulk Chemicals from Renewable Resources-The Potential of White Biotechnology*, The BREW Project report, European Commissions Growth Programme, **2006**; c) S. Van de Vyver, J. Geboers, P. A. Jacobs, B. F. Sels, *ChemCatChem* **2011**, *3*, 82-94; d) M. Rose, R. Palkovits, *Macromol. rapid commun.* **2011**, *32*, 1299-1311; e) D. M. Alonso, J. Q. Bond, J. A. Dumesic, *Green Chem.* **2010**, *12*, 1493-1513; f) S. Li, W. Deng, S. Wang, P. Wang, D. An, Y. Li, Q. Zhang, Y. Wang, *ChemSusChem* **2018**, *11*, 1995-2028; g) Z. Sun, B. Fridrich, A. de Santi, S. Elangovan, K. Barta, *Chem. Rev.* **2018**, *118*, 614-678; h) L. T. Mika, E. Csefalvay, A. Nemeth, *Chem. Rev.* **2018**, *118*, 505-613.
- [5] a) P. N. R. Vennestrøm, C. M. Osmundsen, C. H. Christensen, E. Taarning, *Angew. Chem. Int. Ed.* **2011**, *50*, 10502-10509; b) M. Pelckmans, T. Renders, S. Van de Vyver, B. F. Sels, *Green Chem.* **2017**, *19*, 5303-5331; c) C. G. S. Lima, J. L. Monteiro, T. de Melo Lima, M. Weber Paixao, A. G. Correa, *ChemSusChem* **2018**, *11*, 25-47; d) K. Gupta, R. K. Rai, S. K. Singh, *ChemCatChem* **2018**, *10*, 2326-2349.
- [6] a) L. Yan, Q. Yao, Y. Fu, *Green Chem.* **2017**, *19*, 5527-5547; b) F. D. Pileidis, M. M. Titirici, *ChemSusChem* **2016**, *9*, 562-582.
- [7] a) D. W. Rackemann, W. O. S. Doherty, *Biofuels, Bioprod. Biorefin.* **2011**, *5*, 198-214; b) A. Szabolcs, M. Molnar, G. Dibo, L. T. Mika, *Green Chem.* **2013**, *15*, 439-445; c) J. J. Bozell, L. Moens, D. C. Elliott, Y. Wang, G. G. Neuenschwander, S. W. Fitzpatrick, R. J. Bilski, J. L. Jarnefeld, *Resour. Conserv. Recycl.* **2000**, *28*, 227-239; d) S. M. Kang, J. X. Fu, G. Zhang, *Renew. Sustain. Energy Rev.* **2018**, *94*, 340-362.
- [8] B. V. Timokhin, V. A. Baransky, G. D. Eliseeva, *Russ. Chem. Rev.* **1999**, *68*, 73-84.
- [9] a) J. J. Bozell, G. R. Petersen, *Green Chem.* **2010**, *12*, 539-554; b) A. Aden, J. Bozell, J. Holladay, J. White, A. Manheim, in *Top Value Added Chemicals from Biomass Volume I, Results of Screening for Potential Candidates from Sugars and Synthesis Gas*, U.S. Department of Energy (DOE) Report, **2004**.
- [10] a) S. Selifonov, Glycerol levulinate ketals and their use in the manufacture of polyurethanes, polyurethanes formed therefrom, US Patent 0196947A1, 2012; b) A. S. Amarasekara, S. A. Hawkins, *Eur. Polym. J.* **2011**, *47*, 2451-2457.
- [11] Y. Guo, K. Li, J. H. Clark, *Green Chem.* **2007**, *9*, 839-841.
- [12] a) A. Démolis, N. Essayem, F. Rataboul, *ACS Sustainable Chem. Eng.* **2014**, *2*, 1338-1352; b) S. Saravanamurugan, A. Riisager, *ChemCatChem* **2013**, *5*, 1754-1757; c) Q. J. Luan, L. J. Liu, S. W. Gong, J. Lu, X. Wang, D. M. Lv, *Process Saf. Environ. Prot.* **2018**, *117*, 341-349.
- [13] a) J. Q. Bond, D. M. Alonso, D. Wang, R. M. West, J. A. Dumesic, *Science* **2010**, *327*, 1110-1114; b) D. M. Alonso, J. Q. Bond, J. C. Serrano-Ruiz, J. A. Dumesic, *Green Chem.* **2010**, *12*, 992-999; c) S. Lomate, A. Sultana, T. Fujitani, *Catal. Lett.* **2018**, *148*, 348-358.
- [14] a) A. S. Amarasekara, T. B. Singh, E. Larkin, M. A. Hasan, H.-J. Fan, *Ind. Crops Prod.* **2015**, *65*, 546-549; b) G. Liang, A. Wang, X. Zhao, N. Lei, T. Zhang, *Green Chem.* **2016**, *18*, 3430-3438.
- [15] Y. Z. Qin, M. H. Zong, W. Y. Lou, N. Li, *ACS Sustain. Chem. Eng.* **2016**, *4*, 4050-4054.
- [16] K. M. Doll, S. Z. Erhan, *Green Chem.* **2008**, *10*, 712-717.
- [17] a) W. Wang, N. Li, S. Li, G. Li, F. Chen, X. Sheng, A. Wang, X. Wang, Y. Cong, T. Zhang, *Green Chem.* **2016**, *18*, 1218-1223; b) J. Xin, S. Zhang, D. Yan, O. Ayodele, X. Lu, J. Wang, *Green Chem.* **2014**, *16*, 3589-3595.
- [18] a) Y.-B. Huang, J.-J. Dai, X.-J. Deng, Y.-C. Qu, Q.-X. Guo, Y. Fu, *ChemSusChem* **2011**, *4*, 1578-1581; b) A. Ledoux, L. Sandjong Kuigwa, E. Framery, B. Andrioletti, *Green Chem.* **2015**, *17*, 3251-3254.
- [19] a) F. Liguori, C. Moreno-Marrodon, P. Barbaro, *ACS Catal.* **2015**, *5*, 1882-1894; b) S. Gundekari, K. Srinivasan, *Appl. Catal. A: Gen.* **2019**, *569*, 117-125.
- [20] D. M. Alonso, S. G. Wettstein, J. A. Dumesic, *Green Chem.* **2013**, *15*, 584-595.
- [21] a) B. M. Trost, J. R. Corte, *Angew. Chem. Int. Ed.* **1999**, *38*, 3664-3666; b) B. M. Trost, J. R. Corte, M. S. Gudiksen, *Angew. Chem. Int. Ed.* **1999**, *38*, 3662-3664; c) W. C. C. Bernhart, P. Gautier, *Derivatives of  $\gamma$ -butyrolactone with an anti-arrhythmic activity and compositions*, US Patent 4,542,134, **1985**; d) H.-F. Chan, *The preparation of substituted gamma butyrolactones useful as intermediates for making fungicidal imidazoles and triazoles*, European Patent 0162265 B1, **1990**.
- [22] a) C. Stone, *Use of gamma substituted gamma-butyrolactone to increase levels of their corresponding substituted gamma-hydroxybutyrate derivatives in humans*, US Patent 0132846 A1, **2002**; b) T. Dohi, N. Takenaga, A. Goto, A. Maruyama, Y. Kita, *Org. Lett.* **2007**, *9*, 3129-3132; c) J. D. Lambert, J. E. Rice, J. Hong, Z. Hou, C. S. Yang, *Bioorg. Med. Chem. Lett.* **2005**, *15*, 873-876; d) A. Albrecht, J. F. Koszok, J. Modranka, M. Rózsalski, U. Krajewska, A. Janecka, K. Studzian, T. Janecki, *Bioorg. Med. Chem.* **2008**, *16*, 4872-4882; e) C.-C. Tzeng, K.-H. Lee, T.-C. Wang, C.-H. Han, Y.-L. Chen, *Pharm. Res.* **2000**, *17*, 715-719.
- [23] a) J. Cejka, A. Corma, S. Zones, in *Handbook of Zeolites and Catalysis: Synthesis, Reactions and Applications*, Wiley-VCH Verlag GmbH & Co. KGaA, **2010**; b) R. A. Sheldon, I. Arends and U. Hanefeld, in *Handbook of Green chemistry and Catalysis*, Wiley-VCH Verlag GmbH & Co. KGaA, **2007**.
- [24] a) T. P. Vispute, H. Zhang, A. Sanna, R. Xiao, G. W. Huber, *Science* **2010**, *330*, 1222-1227; b) E. I. Gürbüz, J. M. R. Gallo, D. M. Alonso, S. G. Wettstein, W. Y. Lim, J. A. Dumesic, *Angew. Chem. Int. Ed.* **2013**, *52*, 1270-1274; c) Q. Guo, F. Fan, E. A. Pidko, W. N. P. van der Graaff, Z. Feng, C. Li, E. J. M. Hensen, *ChemSusChem* **2013**, *6*, 1352-1356; d) E. Taarning, C. M. Osmundsen, X. Yang, B. Voss, S. I. Andersen, C. H. Christensen, *Energy Environ. Sci.* **2011**, *4*, 793-804; e) S. Saravanamurugan, M. Paniagua, J. A. Melero, A. Riisager, *J. Am. Chem. Soc.* **2013**, *135*, 5246-5249; f) W. Luo, U. Deka, A. M. Beale, E. R. H. van Eck, P. C. A. Bruijincx, B. M. Weckhuysen, *J. Catal.* **2013**, *301*, 175-186; g) P. Bhanja, A. Bhaumik, *Fuel* **2016**, *185*, 432-441.
- [25] J. C. Jansen, E. J. Creyghton, S. L. Njo, H. van Koningsveld, H. van Bekkum, *Catal. Today* **1997**, *38*, 205-212.
- [26] S. Gundekari, K. Srinivasan, *Catal. Lett.* **2018** (DOI: 10.1007/s10562-018-2618-7).

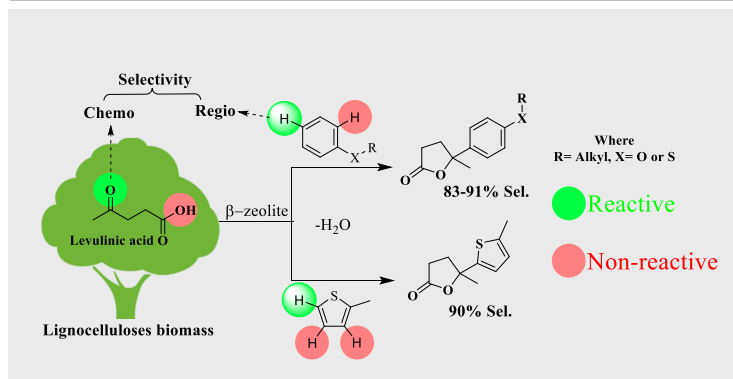
## FULL PAPER

- 1 [27] M. Varkolu, R. Chakali, V. P. Chodimella, D. R. Burri, R. R.  
2 S. Kamaraju, *RSC Adv.* **2014**, *4*, 9660-9668.
- 3 [28] a) O. A. Baturina, S. R. Aubuchon, K. J. Wynne, *Chem. Mater.*  
4 **2006**, *18*, 1498-1504; b) W.-F. Chiang, H.-Y. Fang, C.-H. Wu,  
5 C.-J. Huang, C.-Y. Chang, Y.-M. Chang, C.-L. Chen, *J. Air*  
6 *Waste Manage. Assoc.* **2009**, *59*, 148-154; c) V. Halperin, G.  
7 E. Shter, V. Gelman, D. M. Peselev, M. Mann-Lahav, G. S.  
8 Grader, *Catal. Sci. Technol.* **2015**, *5*, 1153-1162; d) J.  
9 Adelene Nisha, M. Yudasaka, S. Bandow, F. Kokai, K.  
10 Takahashi, S. Iijima, *Chem. Phys. Lett.* **2000**, *328*, 381-386;  
11 e) A. Devaraj, M. Vijayakumar, J. Bao, M. F. Guo, M. A.  
12 Derewinski, Z. Xu, M. J. Gray, S. Prodingler, K. K. Ramasamy,  
13 *Sci. Rep.* **2016**, *6*, 37586; f) Y. Luo, Z. Wang, Y. Fu, C. Jin,  
14 Q. Wei, R. Yang, *J. Mater. Chem. A* **2016**, *4*, 12583-12590;  
15 g) E. Fiamegkou, E. Kollia, A. Vavouliotis, V. Kostopoulos, *J.*  
16 *Compos. Mater.* **2015**, *49*, 3241-3250; h) Z. Wang, M. Liu, X.  
17 Cheng, Y. He, Y. Hu, C. Ma, in *International Journal of*  
18 *Chemical Reactor Engineering*, Vol. 16, **2018**.
- 19 [29] a) P. Castaño, G. Elordi, M. Olazar, A. T. Aguayo, B.  
20 Pawelec, J. Bilbao, *Appl. Catal. B* **2011**, *104*, 91-100; b) A.  
21 R. Pradhan, T.-S. Lin, W.-H. Chen, S.-J. Jong, J.-F. Wu, K.-  
22 J. Chao, S.-B. Liu, *J. Catal.* **1999**, *184*, 29-38; c) W.-H. Chen,  
23 A. Pradhan, S.-J. Jong, T.-Y. Lee, I. Wang, T.-C. Tsai, S.-B.  
24 Liu, *J. Catal.* **1996**, *163*, 436-446.
- 25 [30] a) S. Al-Khattaf, C. D'Agostino, M. N. Akhtar, N. Al-Yassir, N.  
26 Y. Tan, L. F. Gladden, *Catal. Sci. Technol.* **2014**, *4*, 1017-  
27 1027; b) K. Barbera, S. Sørensen, S. Bordiga, J. Skibsted, H.  
28 Fordsmand, P. Beato, T. V. W. Janssens, *Catal. Sci. Technol.*  
29 **2012**, *2*, 1196-1206; c) P. Shestakova, C. Martineau, V.  
30 Mavrodinova, M. Popova, *RSC Adv.* **2015**, *5*, 81957-81964.
- 31 [31] Z. Zhao, S. Xu, M. Y. Hu, X. Bao, C. H. F. Peden, J. Hu, *The*  
32 *J. Phys. Chem. C* **2015**, *119*, 1410-1417.
- 33 [32] a) A. M. R. Galletti, C. Antonetti, V. De Luise, M. Martinelli,  
34 *Green Chem.* **2012**, *14*, 688-694; b) W. R. H. Wright, R.  
35 Palkovits, *ChemSusChem* **2012**, *5*, 1657-1667.
- 36 [33] a) A. M. Camiloti, S. L. Jahn, N. D. Velasco, L. F. Moura, D.  
37 Cardoso, *Appl. Catal. A* **1999**, *182*, 107-113; b) J. C. Lee, J.  
38 Y. Yuk, S. H. Cho, *Synth. Commun.* **1995**, *25*, 1367-1370.
- 39  
40  
41  
42  
43  
44  
45  
46  
47  
48  
49  
50  
51  
52  
53  
54  
55  
56  
57  
58  
59  
60  
61  
62  
63  
64  
65

## FULL PAPER

## Entry for the Table of Contents

## FULL PAPER



Sreedhar Gundekar<sup>[a, b]</sup>, Kannan Srinivasan<sup>[a, b]</sup>

Page No. – Page No.

**Chemo- and regioselective synthesis of arylated  $\gamma$ -valerolactones from bio-based levulinic acid with aromatics using H- $\beta$  zeolite catalyst**

### H- $\beta$ catalysed chemo- and regioselective synthesis of arylated $\gamma$ -valerolactones

Herein, we report preparation of arylated  $\gamma$ -valerolactones for the first time from bio-based levulinic acid with aromatics using recyclable H- $\beta$  zeolite catalyst under solvent free conditions with good selectivity.